Food Chemistry: X 22 (2024) 101267

Contents lists available at ScienceDirect

Food Chemistry: X

journal homepage: www.sciencedirect.com/journal/food-chemistry-x

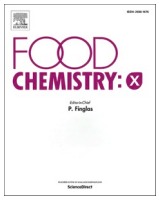

Flow field-flow fractionation coupled with multidetector: A robust approach for the separation and characterization of resistant starch

Mu Wang [a,1], Wenhui Zhang [a,1], Liu Yang [a], Yueqiu Li [a], Hailiang Zheng [b,*], Haiyang Dou [a,c,d,*]

[a] Key Laboratory of Pathogenesis Mechanism and Control of Inflammatory-Autoimmune Disease of Hebei Province, College of Basic Medical Sciences, Hebei University, Baoding 071000, China
[b] Clinical Laboratory, Affiliated Hospital of Hebei University, Baoding 071000, China
[c] State Key Laboratory of New Pharmaceutical Preparations and Excipients, Hebei University, Baoding 071002, China
[d] Key Laboratory of Medicinal Chemistry and Molecular Diagnosis of Ministry of Education, Hebei University, Baoding 071002, China

ARTICLE INFO

Keywords:
Resistant starch
Flow field-flow fractionation
Characterization

ABSTRACT

The unique properties of resistant starch (RS) have made it applicable in the formulation of a broad range of functional foods. The physicochemical properties of RS play a crucial role in its applications. Recently, flow field-flow fractionation (FlFFF) has attracted increasing interest in the separation and characterization of different categories of RS. In this review, an overview of the theory behind FlFFF is introduced, and the controllable factors, including FlFFF channel design, sample separation conditions, and the choice of detector, are discussed in detail. Furthermore, the applications of FlFFF for the separation and characterization of RS at both the granule and molecule levels are critically reviewed. The aim of this review is to equip readers with a fundamental understanding of the theoretical principle of FlFFF and to highlight the potential for expanding the application of RS through the valuable insights gained from FlFFF coupled with multidetector analysis.

1. Introduction

Resistant starch (RS) is defined by the Food and Agriculture Organization (FAO) in accordance with the recommendations of Englyst and EURESTA (European Food-Linked Agro-Industrial Research-Concerted Action on Resistant Starch) as the starches and their degradation products that remain unabsorbed in the small intestine of healthy individuals (Asp, 1992). RS is categorized into five distinct groups (RS1-RS5) based on its morphology and physicochemical properties (Table 1) (Brown, 1996; Englyst, Kingman, & Cummings, 1992; Evans, 2016). RS exhibits dietary fiber functional properties, including prevention of gastrointestinal and cardiovascular diseases, improvement of immunity, and enhancement of mineral absorption. RS has been applied in the food industry, medical care, material science, and other fields (Fig. 1) (Hernandez-Hernandez, Julio-Gonzalez, Doyagüez, & Gutiérrez, 2023; Liang et al., 2023; Tekin & Dincer, 2023; Thongsomboon, Srihanam, & Baimark, 2023; Wang et al., 2023; Wen, Li, & Nie, 2023).

Starch consists of homogeneous glucan components: amylose (AM), mainly linear chains with a molecular weight (M_w) of approximately 10^5–10^6, and amylopectin (AP), branched chains with M_w of approximately 10^7–10^9 (Lu, Zhu, Bao, Liu, Yu, & Chen, 2020; Tester, Karkalas, & Qi, 2004). Several factors affect RS content in starch, including AM content, plant genotypes and mutations, the physical form of grains and seeds, the size of starch granules and molecules, and food processing techniques (Lopez-Silva, Bello-Perez, Castillo-Rodriguez, Agama-Acevedo, & Alvarez-Ramirez, 2020; Ma, Yin, Hu, Li, Liu, & Boye, 2018; Yee et al., 2021). Among these factors, the characteristics of starch granules (such as AM/AP ratio, crystal structure, and gelatinization) play a vital role in evaluating the digestive properties and functional mechanisms of RS (Ding, Luo, & Lin, 2019; Gong, Cheng, Gilbert, & Li, 2019). French (1984) investigated the crystal structure of starch granules by the X-ray diffraction (XRD) technique. Three possible crystalline structures of starch granules were identified by XRD: type A, type B, and type C. Type A starch contains a digestible additional spiral in the center of its hexagonal array (Imberty, Chanzy, Pérez, Buléon, & Tran, 1987), while type B starch has water occupying the central hexagonal array, making it difficult to digest (Brown, 1996). Type C starch is considered the combination of type A and type B crystallization and has resistance

* Corresponding authors at: Key Laboratory of Pathogenesis Mechanism and Control of Inflammatory-Autoimmune Disease of Hebei Province, College of Basic Medical Sciences, Hebei University, Baoding 071000, China (H. Dou).
E-mail addresses: adam0311@hbu.edu.cn (H. Zheng), douhaiyang-1984@163.com (H. Dou).
[1] These authors contributed equally to this study.

https://doi.org/10.1016/j.fochx.2024.101267
Received 25 November 2023; Received in revised form 28 February 2024; Accepted 29 February 2024
Available online 1 March 2024

Table 1
Classification of resistant starch and structural characteristics of resistance to enzymatic digestion.

Classification of RS	Structure affecting digestion	Reference
Physically inaccessible starch (RS1)	Starch granules encased by a thick cell wall and matrix	(Brown, 1996)
Non-gelatinized starch granules (RS2)	Semicrystalline properties of starch granules, susceptibility of the granules to gelatinization	(Gallant, Bouchet, Buléon, & Pérez, 1992)
Retrograded starch (RS3)	The more orderly internal structure of the rearranged starch with stable hydrogen bonds	(Englyst, Kingman, & Cummings, 1992)
Chemically modified starch (RS4)	High hydrophobicity, increased intergranular connections density, crosslinks, and steric hindrance	(Dong & Vasanthan, 2020)
Starch complex (RS5)	Helical molecular structure formed by amylose and long branched chains of amylopectin bound with different substances	(Panyoo & Emmambux, 2017)

to enzymatic hydrolysis. Another significant factor affecting the resistance of natural starch granules to enzymatic hydrolysis is the sensitivity to gelatinization. Gelatinization can lead to the breakdown and dissolution of the compact crystal structure of starch granules, making them more susceptible to digestion by enzymes. Although the AOAC (Association of Official Analytical Communities) method is commonly used for determining RS content, it cannot provide structural insights into RS. Recently, Guo et al. (2022) developed a novel approach for the structural characterization and quantitative analysis of RS by offline coupling of asymmetrical flow field-flow fractionation (AF4) and liquid chromatography (LC). The results showed that the digestibility of starch is closely related to its crystal structure. The AM molecules in type C starch play a crucial role in the anti-digestion process. The results demonstrated that AF4 × LC is a powerful method for informative structural detection and quantitative analysis of RS over its entire M_w distribution.

Size exclusion chromatography (SEC), fluorophore-assisted carbohydrate electrophoresis (FACE), and high performance anion exchange chromatography (HPAEC) are commonly used to characterize starch (Gilbert, Witt, & Hasjim, 2013). HPAEC coupled with a pulsed amperometric detector (PAD) can provide information on the chain length distribution (CLD) of starch (Li, Li, & Gilbert, 2019). Longer CLDs are associated with a more ordered physical structure, especially in retrograded starches (RS3), which contributes to higher resistance to enzymatic digestion (Zhu & Liu, 2020). SEC, a size-based separation method, can be used to separate AM and AP molecules. Furthermore, SEC coupled with multiangle light scattering (MALS) is commonly used to determine the M_w and radius of gyration (R_g) distributions of the starch components (Bello-Perez, Agama-Acevedo, Lopez-Silva, & Alvarez-Ramirez, 2019). However, obtaining an accurate detection of AP molecules can be challenging due to column adsorption and shear degradation of AP molecules (Cave, Seabrook, Gidley, & Gilbert, 2009). Flow field-flow fractionation (FlFFF) is a valuable technique for separating starch with ultrahigh M_w due to its rapid and gentle separation

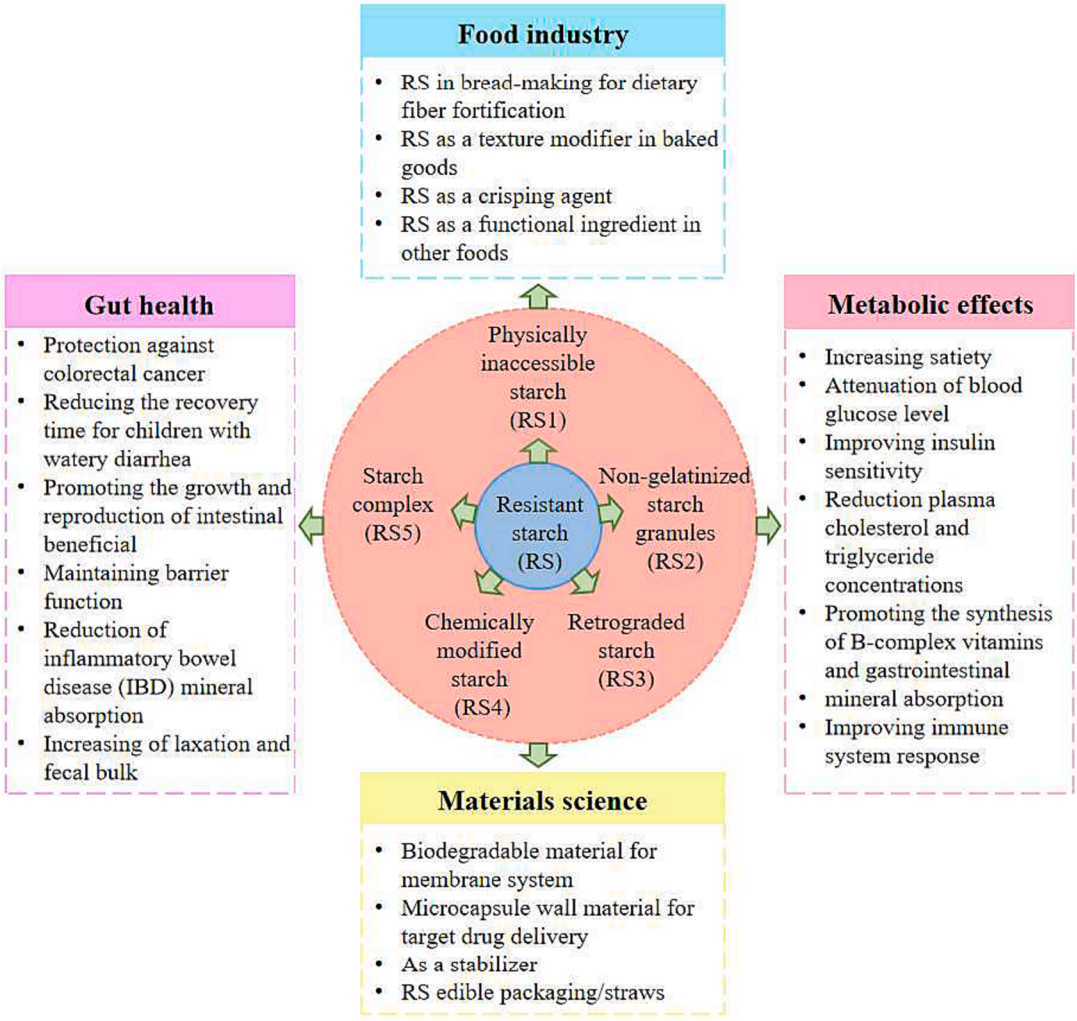

Fig. 1. Classification and application of RS.

mechanism (Giddings, 1966). Notably, FlFFF lacks a stationary phase and packing material in the channel, which minimizes shear degradation risks, especially for AP molecules (González-Espinosa, Sabagh, Moldenhauer, Clarke, & Goycoolea, 2019). FlFFF coupled with online MALS and differential refractive index (dRI) detectors can provide the entire size distribution and molecular conformation information about RS (Zhang, Shen, Song, Chen, Zhang, & Dou, 2021). Wahlund et al. (2011) studied a wide range of starches from different plant sources by AF4-MALS-dRI. The results showed that the relative quantity, M_w, R_g, and hydrodynamic diameter (d_h) of starch molecules from different plant sources and varieties varied greatly. AF4-MALS-dRI has been proven to be a valuable tool for characterizing RS.

In a previous review, the dissolution, structure, and functions of starch characterized by AF4-MALS-dRI were summarized (Guo, Li, An, Shen, & Dou, 2019). Compared to SEC, FlFFF analysis of starches involves a greater number of controllable factors. To our knowledge, there is a notable absence of comprehensive reviews on the separation and characterization of RS by using FlFFF. In this review, the theory of FlFFF and the controllable factors affecting the sample separation of FlFFF are introduced in detail. The applications of FlFFF in the separation and characterization of RS are critically reviewed.

2. Flow field-flow fractionation (FlFFF)

FlFFF, an important sub-technique of field-flow fractionation, was proposed by Giddings in 1976. FlFFF has the widest separation range and the best compatibility with various carrier liquids, supporting extensive applications to multi-sized analytes from diverse sources (Wu et al., 2023). In this review, the theory and operation modes and the variant of FlFFF are reviewed.

2.1. Principle of flow field-flow fractionation (FlFFF)

In FlFFF, a ribbon-like separation channel (as shown in Fig. 2(a)) is usually assembled by sandwiching a thin spacer between two blocks (top and base in Fig. 2(b)). The shape of the spacer determines the shape of the FlFFF separation channel. In the FlFFF channel, the fluid can be approximated as a Poiseuille flow between two infinite planes, and the flow phase velocity distribution within the separation channel can be approximated as a parabolic flow profile (Fig. 2(c)). From the edge of the channel to its center, the flow velocity of the fluid gradually increases and reaches a maximum at the centerline. An applied external force, called cross-flow, is introduced in the direction perpendicular to the separation channel, which persists throughout the separation process. When the sample is injected into the separation channel, the sample particles accumulate on its bottom wall (acting as an accumulation wall) under the combined action of the applied external force and its own diffusion force. When the applied external force is balanced with the diffusion force of the particles, the samples can be separated in the channel. FlFFF maintains the integrity of the structure and properties of the sample, and the collected fractions can be further analyzed online or offline using other characterization methods (e.g., ultraviolet (UV),

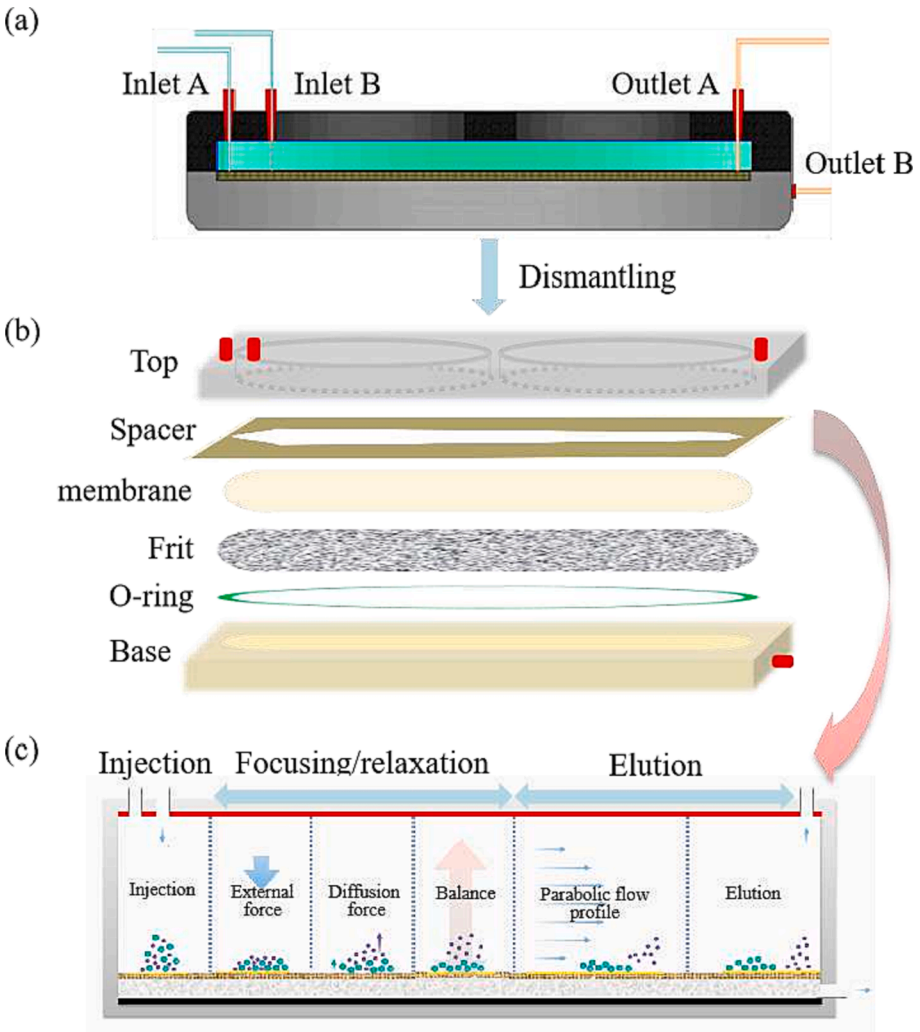

Fig. 2. Schematic diagram of the channel (a and b) and separation process (c) of FlFFF.

fluorescence, dRI, MALS, etc.).

2.2. Variants of flow field-flow fractionation (FlFFF)

Several variants of FlFFF have been developed, each with different characteristics as summarized in Table 2. Symmetrical FlFFF (SF4) channel has a permeable top wall, and the flow conditions are set at low flow rates with identical inlet and outlet flow velocities. However, SF4 presented certain challenges, including prolonged injection time, peak broadening, and low resolution (Giddings, Yang, & Myers, 1977). It was improved by AF4 (Wahlund & Giddings, 1987; Wahlund, Winegarner, Caldwell, & Giddings, 1986). In AF4, the top wall of the channel is impermeable, and the bottom wall is permeable, allowing the cross-flow to pass through the channel. Subsequently, the trapezoidal asymmetrical parallel plate channel (TrAF4) was developed (Litzen, 1993; Litzen & Wahlund, 1991). AF4 is suitable for the characterization of synthetic and natural polymers, including proteins and polysaccharides. In addition to soluble polymers, AF4 can separate colloidal particles in the range of approximately 1 nm to 1 μm in diameter (in the normal mode) (Podzimek, 2012).

Hollow fiber FlFFF (HF5) was developed with some advantages such as low sample loading, high sensitivity, short analysis time, and potential disposability (Joensson & Carlshaf, 1989). However, it is worth noting that low sample loading and disposability also represent disadvantages for this method. To solve the overloading effect observed with HF5, the tandem HF5 approach was developed to enhance the detection of low abundance components (Zattoni, Rambaldi, Casolari, Roda, & Reschiglian, 2011). Commercially manufactured AF4 instruments equipped with frit inlet and frit outlet channel came into existence in the 1990s. The key advantage of the frit inlet FlFFF channel is the elimination of the focusing step, enabling a higher injection mass compared to a conventional channel, thereby mitigating the risk of sample overloading (Fuentes, Choi, Zielke, Peñarrieta, Lee, & Nilsson, 2019). The frit outlet FlFFF channel enhances mass detection sensitivity (Clark & Zika, 2001).

2.3. Elution modes of flow field-flow fractionation (FlFFF)

The sample separation in FlFFF occurs within a ribbon-like channel. According to the elution order of the samples, elution modes of FlFFF are categorized into normal mode and steric/hyperlayer mode (Fig. 3).

2.3.1. Normal mode

The field force (F_F) employed in FlFFF makes the sample components spread uniformly to the accumulation wall, which is expressed as Eq. (1) (Giddings, Ratanathanawongs, & Moon, 1991):

Table 2
Characteristics of FlFFF variants.

FlFFF variant	Characteristic	Reference
Symmetrical FlFFF (SF4)	Low flow conditions, stop-flow relaxation period	(Giddings, Yang, & Myers, 1977)
Asymmetrical FlFFF (AF4)	Most used, high resolution	(Wahlund & Giddings, 1987)
Hollow fiber FlFFF (HF5)	Low sample loading, high sensitivity due to lower dilution, short analysis time, potentially disposable	(Joensson & Carlshaf, 1989)
Frit inlet FlFFF	On-the-fly sample relaxation so no stop-flow or focusing flow step, generally lower separation resolution than AF4, good for samples prone to undesirable interactions with the membrane accumulation wall	(Fuentes, Choi, Zielke, Peñarrieta, Lee, & Nilsson, 2019)
Frit outlet FlFFF	Enhancement in detector signal intensity due to lower dilution	(Clark, & Zika, 2001)

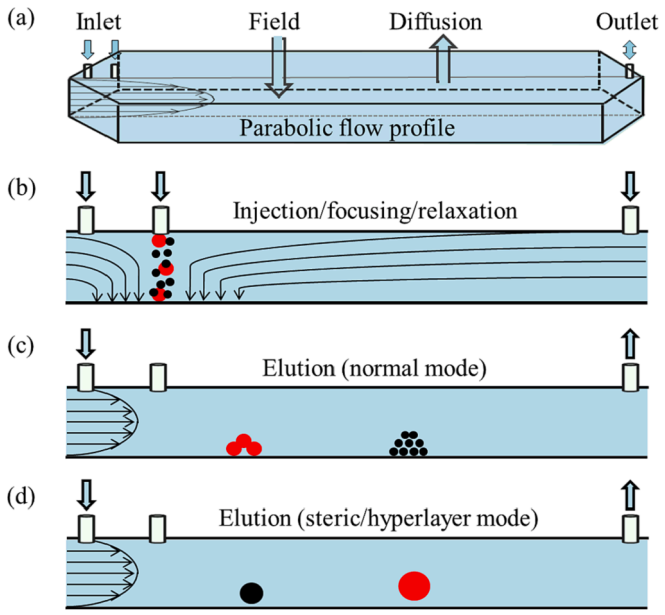

Fig. 3. Main separation modes of FlFFF.

$$F_F = \frac{3\pi\eta d_h w V_c}{V^0} \quad (1)$$

where η is the viscosity of the carrier liquid, d_h is the hydrodynamic diameter of the particle, V_c is the cross-flow rate, w is the channel thickness, and V^0 is the void volume. Eq. (1) shows that F_F is proportional to V_c. At the same time, the sample components diffuse away from the accumulation wall under the action of Brownian motion and finally form an equilibrium layer between the two opposing transport processes. For the sample with d_h smaller than 1 μm, separation occurs in the normal mode, and retention time (t_r) is inversely proportional to the diffusion coefficient D and proportional to d_h (Ratanathanawongs Williams & Lee, 2006). The carrier liquid enters the channel from the inlet and forms a parabolic profile inside the channel, with the highest velocity at the center of the channel (Fig. 3). As a result, the smaller particles are eluted earlier than larger ones, which is the so-called normal mode, as shown in Fig. 3(c).

2.3.2. Steric/hyperlayer mode

As the sample diameter increases, the elution mode shifts from the normal mode to the steric/hyperlayer mode with an opposite elution order (Kim, Yang, & Moon, 2018). When the particle size is larger than 1 μm, the diffusion force of the particle can be ignored. In this case, the particles are driven downward by the F_F to (or close to) the accumulation wall, where the centers of the large particles are in a faster stratosphere and then are eluted first (Fig. 3(d)) (Giddings, 1993; Myers & Giddings, 1982). When the force of hydrodynamic lift (F_{HL}) is sufficient to counteract the F_F, a particle-focusing layer is formed at a distance from the accumulation wall (Mélin et al., 2012). F_{HL} is caused by inertia and other factors of liquid carriers (Reschiglian et al., 2000). There is the "steric transition" phenomenon when the sample elution mode changes from the normal mode to the steric/hyperlayer mode (Dou, Lee, Jung, Lee, & Lee, 2013; Kim, Yang, & Moon, 2018). When the sample's size range spans the steric transition region (i.e., the particle size range overlaps between the normal mode and steric/hyperlayer mode), it can lead to simultaneous elution of particles with different sizes. This makes it challenging to determine the accurate size distribution of the sample components (Dou, Jung, & Lee, 2015; Perez-Rea, Zielke, & Nilsson, 2017; Zielke, Fuentes, Piculell, & Nilsson, 2018). The particles with large size are generally formed during starch retrogradation process. Therefore, when FlFFF is employed for the separation of RS3, great care

is needed, as steric phenomenon may occur (Zhang et al., 2019).

2.4. Resolution and retention ratio in flow field-flow fractionation (FlFFF)

Resolution (R_s) is one term for evaluating the separation efficiency between two analyte components. During the separation process of two components, two distinct types of dispersion need to be considered: selective dispersion (Δt_r) and random dispersion (Schimpf, Myers, & Giddings, 1987). Δt_r is beneficial to the separation of two components, whereas random dispersion is not. Δt_r is quantified by the selectivity (S), which reflects the difference in retention volume (or t_r) with M_w or particle diameter. Random dispersion is quantified by plate height (H). Therefore, the resolution depends on both H and S, and can be expressed as Eq. (2):

$$R_s = \frac{\Delta z}{2(\sigma_1 + \sigma_2)} = \frac{\Delta z}{4\bar{\sigma}} \tag{2}$$

where Δz is the gap between the centers of gravity of neighboring zones and σ is the standard deviation of the zones. The subscripts on σ refer to components 1 and 2, and $\bar{\sigma}$ refers to an average value for two zones. Consequently, Δz reflects selective dispersion, while σ indicates the extent to which the gap is filled by cross-contamination due to random dispersion. It is well known that the M_w of AM and AP molecules has an overlap (Dou, Zhou, Jang, & Lee, 2014; Zhang et al., 2019). Thus, a baseline separation for starch samples by FlFFF is still a challenge.

The retention ratio (R) is defined as the ratio of the times associated with the void time and retention time, and it is expressed as Eq. (3):

$$R = 6\gamma\alpha(1-\alpha) + \left[\left(1-2\alpha\right)coth\left(\frac{1-2\alpha}{2\lambda}\right) - 2\lambda\right] \tag{3}$$

where γ is a dimensionless parameter that depends on the field strength, migration velocity, and particle size (Kim, Yang, & Moon, 2018). α is the ratio of particle radius (a) to w, λ is the ratio of the mean layer thickness (l) to w, which can be expressed as (Wahlund & Giddings, 1987):

$$\lambda = \frac{kTV^0}{3\pi\eta w^2 d_h V_c} \tag{4}$$

where k is the Boltzmann constant and T is the absolute temperature. When λ is very small, Eq. (3) can be reduced to Eq. (5):

$$R = 6\gamma\alpha + 6\lambda \tag{5}$$

In the Eq. (5), the first term of the equation is proportional to the particle size, while the second term is inversely proportional to the particle size. As a result, R decreases with increasing d_h and reaches the minimum value (R_i). The diameter corresponding to R_i is called the "steric transition point" (d_i). d_i and R_i are expressed as Eqs. (6) and (7), respectively:

$$d_i = \sqrt{\frac{2kTV^0}{3\pi\eta w\gamma V_c}} \tag{6}$$

and

$$R_i = \frac{6\gamma d_i}{w} \tag{7}$$

For highly retained components in FlFFF ($l \ll w$ or $\lambda \to 0$), Eq. (5) can be approximated to yield a so-called "simplified" retention equation (Eq. (8) for the normal mode and Eq. (9) for the steric/hyperlayer mode):

$$R = 6\lambda \tag{8}$$

$$R = 6\gamma\alpha \tag{9}$$

In the normal mode, R is inversely proportional to the particle size, while in the steric/hyperlayer mode, R is proportional to the particle size. The value of γ is related to the information of the elution mode (steric or hyperlayer mode) (Moon & Giddings, 1992). When the sample size ranges in the steric transition region, the elution mode can be adjusted by changing the elution parameters. For FlFFF analysis of polydisperse samples (such as RS), it is crucial to optimize the elution conditions to avoid steric transition.

3. Factors affecting sample separation of flow field-flow fractionation

Despite the excellent separation performance of FlFFF, the retention and accumulation of samples on the surface of the accumulation wall can result in low sample recovery, which may limit the potential applications of this technology. Additionally, the retention capacity of ultrafiltration membranes imposes constraints on the minimum sample size in FlFFF. Therefore, prior to conducting sample separation using FlFFF, a series of parameters need to be optimized to attain ideal separation conditions for the given sample. The primary factors that influence sample separation and characterization in FlFFF include the composition of the separation channel, the conditions used for sample separation, and the sensitivity of the detectors.

3.1. Performance of the FlFFF channel

The channel profile in FlFFF is usually designed with diverse dimensions and shapes (Kang & Moon, 2004). The channel dimensions are described by w, the breadth (b), and the length (L). The w is controlled by the thickness of the spacer. The actual thickness of the FlFFF channel is typically 50 μm smaller than the spacer thickness due to the compression of the semipermeable membrane. In comparison to a rectangular channel, the trapezoidal channel design serves to partially compensate for the reduction in axial flow velocity, resulting from the loss of cross-flow through the membrane. This, in turn, mitigates peak dilution and enhances detector responsiveness. At a consistent cross-flow rate, the actual field force is contingent on the area of the semipermeable wall, comprising the channel length L, the channel breadths b_0 (inlet breadth of trapezoidal FlFFF channel), and b_L (outlet breadth of the trapezoidal FlFFF channel), and the areas of tapered ends. Shorter and/or narrower channels are employed to achieve higher field force, which reduces solvent consumption and enhances sample separation efficiency. The lower size limit is determined by the molecular weight cut off (MWCO) of the membrane, while the upper size limit is assessed by a threshold of 20 % of the FlFFF channel thickness.

Ultrafiltration membranes made of regenerated cellulose (RC), polyether sulfone (PES), and cellulose triacetate (CT) with MWCO of 0.3–100 kDa are commonly employed as accumulation walls in FlFFF. Since smaller monosaccharides and oligosaccharides can pass through the ultrafiltration membrane, oligosaccharides with sizes comparable to the MWCO may be blocked in the pores of the ultrafiltration membrane, and large starch molecules can interact with the membrane through chemical (adsorption) or physical (rough surface) interactions, which may result in lower sample recovery and potential membrane contamination. To mitigate these issues, the selection of an appropriate ultrafiltration membrane type and MWCO is crucial to minimize the interactions between the sample and the surface of the membrane, which can ensure a higher sample recovery. In practical applications, when dealing with charged samples, it is essential to choose a suitable carrier liquid to eliminate the interaction between the samples and the ultrafiltration membrane (González-Espinosa, Sabagh, Moldenhauer, Clarke, & Goycoolea, 2019).

3.2. Sample separation conditions

Mudalige et al. (2015) reported that sample modification can alter sample retention within FlFFF. In addition to altering the nature of the sample, optimizing the separation conditions of FlFFF (e.g., external

forces, the nature of the carrier liquid, injection mass, and focusing time) can enhance sample recovery.

3.2.1. External force

During the FlFFF separation process, the choice of external force is critical, as a lower external force can lead to decreased R_s, while a higher external force may increase the risk of sample aggregation and interaction with the surface of the membrane. Optimizing the external force is essential to achieve good sample resolution. For heterogeneous samples with a wide size distribution, it is recommended to employ gradient external force to shorten the analysis time. In the FlFFF elution process, the external force action can be categorized into three main modes: constant mode, linear attenuation mode, and exponential attenuation mode. Among them, the combination of exponentially attenuated external force with other external force modes is frequently employed for the separation of starch samples (Ma, Buschmann, & Winnik, 2010).

3.2.2. Selection of carrier liquid

Ideally, the carrier liquid should be compatible with properties of the sample (such as pH and ionic strength) to inhibit the instability of the sample molecules (such as degradation, aggregation, and adsorption) during FlFFF separation (Kammer, Legros, Hofmann, Larsen, & Loeschner, 2011). Generally, it is recommended to use electrolyte solutions with ionic strength and pH conditions similar to those of the sample. Additionally, in some cases, surfactants are needed to maximize sample recovery, and a bactericide (e.g., sodium azide) can be added to prevent bacterial growth. For starch samples from different plant sources, a carrier liquid composed of diluted electrolytes (such as 1–50 mM $NaNO_3$) is recommended (Nilsson, 2013).When separating polysaccharides (such as chitosan complex and dextran), deionized water is sometimes chosen as the carrier liquid (Faucard et al., 2018; Fraunhofer, Jakob, & Vogel, 2018). To separate the mixture of starches and other biomacromolecules, buffer solutions such as acetate buffer, phosphate buffer, and sodium citrate buffer are commonly used as carrier liquids. Ideally, on the premise of ensuring the stability of the sample, a carrier liquid with a pH value that maximizes repulsion between the sample and the surface of the accumulation wall and an appropriate ionic strength to prevent starch aggregation and/or adsorption should be selected.

3.2.3. Injection mass

FlFFF can provide precise sample characterization with relatively small sample amounts, typically approximately 10 μg or less, depending on the sensitivity of the detection method (Caldwell, Brimhall, Gao, & Giddings, 1988). It is important to be aware of the phenomenon of "sample overloading." Sample overloading results in an excessively high concentration of sample components in the concentration region of the accumulation wall. Sample overloading involves multiple concentration-dependent phenomena, which can lead to an unstable retention ratio (increase or decrease) and asymmetrical peak (tail or front). During the elution process, the interaction between samples or between the sample and the surface of the accumulation wall increases, which results in sample aggregation and/or adsorption (Benincasa & Giddings, 1992; Schimpf, Caldwell, & Giddings, 2000). AP with an ultrahigh M_w is particularly susceptible to sample overloading due to chain entanglement and viscosity effects. Arfvidsson and Wahlund (2003) found that a large injection volume with a low sample concentration is superior to using a small injection volume with a high sample concentration. Therefore, the key to avoid sample overloading is to reduce the maximum sample concentration, which can be achieved by decreasing the injected sample mass.

3.2.4. Focusing time

Regarding the focusing time, during the FlFFF injection and focusing process, it is essential to extend the focusing time to enrich the sample. This ensures that the sample concentration surpasses the detection limit of the detector and minimizes peak broadening. If the focusing time is too short, the sample equilibrium layer distribution is wide, and some sample components may elute within the void peak. On the other hand, an excessively long focusing time can increase the interaction between samples and between samples and the surface of the membrane, potentially leading to sample aggregation and excessive retention (Wahlund, 2013). Therefore, selecting an appropriate focusing time is also a crucial factor in the separation and characterization of RS using FlFFF.

3.3. Sensitivity of the detectors

The sensitivity and detection limit of the detector play a crucial role in the accuracy of characterizing samples by FlFFF. AF4 coupled with a mass detector (typically MALS) and a concentration detector (usually dRI) is primarily used for the separation and characterization of starch molecules in the normal mode. AP molecules with higher M_w and viscosity tend to be closer to the accumulation wall during AF4 separation and are prone to absorb on the surface of the accumulation wall. To achieve optimal separation for AP molecules, it is essential to operate at a lower concentration (Chiaramonte, Rhazi, Aussenac, & White, 2012). The intensity of the MALS signal is influenced by both the concentration and the size of the sample components. According to Rayleigh's approximation, the intensity of light scattering by a particle is proportional to the sixth power of the particle's diameter ($I \propto d^6$), making it more challenging to detect scattered light from smaller particles. Consequently, when a mixture of particles with different sizes is present in the suspension, the data tend to be skewed toward larger particle sizes (Doyle & Wang, 2019; Guisbiers et al., 2016). However, MALS signal detection is particularly challenging for AM molecules with a lower t_r due to their smaller size (Yoo, Choi, Zielke, Nilsson, & Lee, 2017). The sample recovery is determined from the ratio of the mass eluted from the separation channel (integration of the dRI signal) to the injected mass (based on the starch content). However, at a lower injection mass, the dRI detector may exhibit a low signal-to-noise ratio, making it difficult to accurately determine sample recovery and M_w. In such cases, averaging multiple injections can be a reliable method to enhance the accuracy of starch characterization (Leeman, Islam, & Haseltine, 2007). This approach can improve the accuracy of quantitative analysis of AM but may not provide detailed M_w and conformational information about AP. Thus, the subsequent improvements of FlFFF technique (such as modified membranes, coupled with precision detection methods) are necessary to address the characterization challenges of AP molecules.

4. Application of FlFFF for the structural characterization of RS

The characterization of starch at both the granule and molecule levels by direct measurement of physicochemical parameters in association with MALS and dRI is a key feature of the FlFFF technique. The information about the RS obtained from FlFFF is outlined in Table 3.

4.1. Physically inaccessible starch (RS1)

Song et al. (2021) utilized AF4-MALS-dRI to separate and characterize starch granules and starch molecules extracted from various plant sources. The AF4 results were validated by a combination of optical microscopy (OM), scanning electron microscopy (SEM), and dynamic light scattering (DLS) techniques. The size distributions of starch granules determined by AF4 were in reasonable agreement with those obtained from OM. However, OM measurement is time-consuming. The results suggested that AF4 is an appropriate method for determining the sizes of starch granules. Meanwhile, the relationships between the size of starch at nano- to microscale and its functional properties (i.e., digestibility, retrogradation, and thermal properties) were studied by Pearson correlation analysis. The results showed that the sizes of starch granules and starch molecules from different plant sources were related to their digestibility.

Table 3
The information about RS obtained from FlFFF.

Source of RS	Type of RS	Type of FlFFF	FlFFF operation condition				Detection	The information gained by FlFFF	Reference
			Carrier liquid	Membrane	Cross-flow rate	Injection mass			
Rice, lotus	RS1	AF4	3 mM NaN_3, 0.35 mM SDS	RC	1.2 → 0.05 mL/min *Half-time* $t_{1/2} = 3$ min	100 μg	UV, MALS, dRI	M_w, R_g	(Song et al., 2021)
Mung bean, yam, banana	RS2	AF4	5 mM $NaNO_3$	RC	1.2 → 0.05 mL/min $t_{1/2} = 3$ min	10 μg	MALS, dRI, LC	M_w, R_g, content of RS	(Guo, Zhang, Sun, Ye, Shen, & Dou, 2022)
Potato	RS2	AF4	3 mM NaN_3, 5 mM $NaNO_3$	RC	1.2 → 0.05 mL/min $t_{1/2} = 3$ min	25 μg	MALS, dRI	M_w, R_g, ρ_{app}, R_g/R_h	(Zhang, Shen, Song, Chen, Zhang, & Dou, 2021)
Maize, wheat, rice potato, tapioca, pea	RS2	AF4	–	RC	1.0 → 0 mL/min $t_{1/2} = 4$ min	40 μg	MALS, dRI	M_w, R_g, R_h	(Wahlund, Leeman, & Santacruz, 2011)
Potato, maize, wheat	RS2	AF4	3 mM NaN_3	–	–	–	MALS, QELS, dRI	M_w, R_g, R_h	(Rolland-Sabaté, Guilois, Jaillais, & Colonna, 2011)
Potato, maize	RS3	AF4	3 mM NaN_3, 50 mM $NaNO_3$	RC	1.4 → 0.05 mL/min $t_{1/2} = 2$ min	100 μg	MALS, dRI	M_w, R_g, ρ_{app}, R_g/R_h	(Zhang et al., 2019)
Wheat	RS3	AF4	–	RC	2.0 → 0.12 mL/min $t_{1/2} = 4$ min	1.25–15 μg	MALS, dRI	M_w, R_g, ρ_{app}, R_g/R_h	(Fuentes, Castañeda, Rengel, Peñarrieta, & Nilsson, 2019)
Maize	RS4	AF4	3 mM NaN_3, 50 mM $NaNO_3$	RC	0.2 mL/min	100 μg	MALS, dRI	M_w	(Lee et al., 2010)
–	RS4	AF4	3 mM NaN_3, 1 M NaCl	RC	1.0 or 2.0 mL/min	40–300 μg	MALS, dRI	M_w, R_g, R_g/R_h	(Wittgren, Wahlund, Andersson, & Arfvidsson, 2002)
Barley	RS4	EAF4	10 mM PBS	RC	2.0 → 0.25 mL/min $t_{1/2} = 3$ min	60 μg	MALS, dRI	M_w, Zeta potential	(Fuentes, Choi, Wahlgren, & Nilsson, 2023)

4.2. Non-gelatinized starch granules (RS2)

Rolland-Sabaté et al. (2011) utilized AF4 coupled with MALS, quasi-elastic light scattering (QELS), and dRI (AF4-MALS-QELS-dRI) to analyze the structure of varying AM/AP ratios and natural starches from different plant sources. The results showed that AF4 could effectively separate AP molecules and obtain more structural information about branched macromolecules. Zhang et al. (2021) explored the capability of AF4-MALS-dRI for monitoring structural and conformational changes in potato starch during enzymatic hydrolysis. The results revealed that the gelatinization process induced a loose and random coil conformation in potato AM molecules, accelerating enzymatic hydrolysis of potato starch. Guo et al. (2022) conducted structural characterization and quantification of RS extracted from various plant sources (i.e., mung bean, yam, and banana) by offline coupling AF4-MALS-dRI with LC. The results demonstrated that the combination of AF4-MALS-dRI and LC is an effective method for rapid, quantitative, and comprehensive structural information detection of RS over the entire M_w distribution.

4.3. Retrograded starch (RS3)

Starch retrogradation is an inevitable transformation during processing and storage, and often accompanies with structural and conformational changes, especially under low-temperature or cooling conditions. Zhang et al. (2019) studied the influence of the plant source, AM/AP ratio, storage conditions (temperature and time), and salt on starch retrogradation by using AF4-MALS-dRI. The results revealed that nitrate ions retarded starch retrogradation behavior by inhibiting the formation of hydrogen bonds between AM molecules. Moreover, the results highlighted the significant role played by small AM aggregates in starch retrogradation and maize AP degradation, offering valuable insights into the mechanism of starch retrogradation. Fuentes et al. (2019a) analyzed the molecular properties (such as M_w, R_g, and apparent density (ρ_{app})) of wheat starch in three different types of bread by AF4-MALS-dRI. The results showed that the higher the water content of the bread was, the higher the R_g, M_w, ρ_{app}, and content of RS. The content of AM in bread may be related to ρ_{app}, suggesting that the content of RS might be related to the difference in structural and conformational properties of starch. Furthermore, the results also indicated that characterizing non-solvent precipitated starch led to insights into how changes in molecular properties may be associated with the presence of RS (Fuentes et al., 2019b).

4.4. Chemically modified starch (RS4)

RS4 can impact its original structure and lead to changes in M_w via chemical alterations. Several methods, including acid hydrolysis, crosslinking, acetylation/esterification, dual modification, and oxidation, have been employed for the chemical modification of starch (Haq et al., 2019). Lee et al. (2010) investigated the effect of carboxymethylation on the M_w and size distribution of corn starch using AF4-MALS-dRI. The results demonstrated that carboxymethylation of starch resulted in a reduction in M_w due to molecular degradation by the alkaline treatment. The results suggested that AF4-MALS-dRI is a useful tool for monitoring the changes in M_w and the size of starch during derivatization. Additionally, Wittgren et al. (2002) explored the M_w of four commercial hydroxypropyl and hydroxyethyl-modified starches using AF4-MALS-dRI. The results highlighted the ability of AF4-MALS-

dRI to provide a rapid size characterization of modified starches. Recently, Fuentes et al. (2023) investigated the capability of electrical asymmetrical flow field-flow fractionation (EAF4) for determining the charge properties over the M_w distribution of barley starch modified with octenyl succinic anhydride (OSA). The results revealed that EAF4 facilitated the estimation of the zeta potential and net charge of OSA-starch. Furthermore, the results suggested that OSA substituents were not evenly distributed at or near the "surface" of the starch, potentially affecting the adsorption behavior and functionality of OSA-starch in emulsions.

4.5. Starch complex (RS5)

RS5 is a starch complex formed by the combination of long branched chains of AM and AP with different nutrients, which prevents digestive enzymes from binding and hydrolyzing starch by forming a helical molecular structure. Several studies have reported that RS5 is formed when AM or AP is processed with fatty acids or fatty alcohols (Panyoo & Emmambux, 2017). Magnusson and Nilsson (2011) studied the interaction between hydrophobically modified starch, with octenyl succinic anhydride (OSA), and α-β-livetin, which is the water-soluble fraction of egg yolk. Although, AF4-UV-MALS-dRI has been proven to be a useful tool for studying the complex of polysaccharides and proteins (Chen et al., 2022), few studies have reported on the application of FlFFF for RS5.

5. Summary and outlook

In summary, FlFFF is a useful tool for the separation of RS that can aid in optimizing the production process of starch and elucidating the factors that contribute to their resistance to enzymatic digestion. Coupling FlFFF with multidetector (such as MALS and dRI detectors) can serve as a powerful tool to comprehensively understand the structure and conformation of RS. The FlFFF channel with a frit outlet could enhance the signal intensity of AP molecules due to lower dilution and achieve structural characterization even at low RS concentrations. Although, AF4-UV-MALS-dRI has shown its capability for the separation and characterization of RS and would open a new avenue for studying RS5, more exploration is needed regarding the structure of RS and its resistance to enzymatic digestion.

CRediT authorship contribution statement

Mu Wang: Writing – original draft, Conceptualization. **Wenhui Zhang:** Writing – original draft, Conceptualization. **Liu Yang:** Visualization. **Yueqiu Li:** Data curation. **Hailiang Zheng:** Writing – review & editing, Project administration. **Haiyang Dou:** Writing – review & editing, Supervision, Funding acquisition.

Declaration of competing interest

The authors declare that they have no known competing financial interests or personal relationships that could have appeared to influence the work reported in this paper.

Data availability

Data will be made available on request.

Acknowledgments

The authors acknowledge the support provided by the Natural Science Foundation of Hebei Province (H2020201295, 202360102030020), the Hebei Province Key Research Projects (22372505D), the Interdisciplinary Research Program of Natural Science of Hebei University (DXK202115), and the Program of Innovation Ability Enhancement of Baoding (2211N012).

References

Arfvidsson, C., & Wahlund, K. G. (2003). Mass overloading in the flow field-flow fractionation channel studied by the behaviour of the ultra-large wheat protein glutenin. *Journal of Chromatography A, 1011*(1–2), 99–109. https://doi.org/10.1016/S0021-9673(03)01145-2

Asp, N. G. (1992). Resistant starch. Proceedings for the 2nd plenary meeting of EURESTA: European FLAIR Concerted Action No. 11 on physiological implications of the consumption of resistant starch in man. *European Journal of Clinical Nutrition, 38*, S1–S148. https://doi.org/10.1021/ac00176a004

Bello-Perez, L. A., Agama-Acevedo, E., Lopez-Silva, M., & Alvarez-Ramirez, J. (2019). Molecular characterization of corn starches by HPSEC-MALS-RI: A comparison with AF4-MALS-RI system. *Food Hydrocolloids, 96*, 373–376. https://doi.org/10.1016/j.foodhyd.2019.04.067

Benincasa, M. A., & Giddings, J. C. (1992). Separation and molecular weight distribution of anionic and cationic water-soluble polymers by flow field-flow fractionation. *Analytical Chemistry, 64*(7), 790–798. https://doi.org/10.1021/ac00031a016

Brown, I. (1996). Complex carbohydrates and resistant starch. *Nutrition Reviews, 54*(11), S115–S119. https://doi.org/10.1111/j.1753-4887.1996.tb03830.x

Caldwell, K. D., Brimhall, S. L., Gao, Y., & Giddings, J. C. (1988). Sample overloading effects in polymer characterization by field-flow fractionation. *Journal of Applied Polymer Science, 36*(3), 703–719. https://doi.org/10.1002/app.1988.070360319

Cave, R. A., Seabrook, S. A., Gidley, M. J., & Gilbert, R. G. (2009). Characterization of starch by size-exclusion chromatography: The limitations imposed by shear scission. *Biomacromolecules, 10*(8), 2245–2253. https://doi.org/10.1021/bm900426n

Chen, X., Tian, Y., Zhang, J., Li, Y., Zhang, W., Zhang, J., & Dou, H. (2022). Study on effects of preparation method on the structure and antioxidant activity of protein-Tremella fuciformis polysaccharide complexes by asymmetrical flow field-flow fractionation. *Food Chemistry, 384*, Article 132619. https://doi.org/10.1016/j.foodchem.2022.132619

Chiaramonte, E., Rhazi, L., Aussenac, T., & White, D. R. (2012). Amylose and amylopectin in starch by asymmetric flow field-flow fractionation with multi-angle light scattering and refractive index detection (AF4–MALS–RI). *Journal of Cereal Science, 56*(2), 457–463. https://doi.org/10.1016/j.jcs.2012.04.006

Clark, C. D., & Zika, R. G. (2001). Frit inlet/frit outlet flow field-flow fractionation: Methodology for colored dissolved organic material in natural waters. *Analytica Chimica Acta, 443*, 171–181. https://doi.org/10.1016/S0003-2670(01)01202-8

Ding, Y., Luo, F., & Lin, Q. (2019). Insights into the relations between the molecular structures and digestion properties of retrograded starch after ultrasonic treatment. *Food Chemistry, 294*, 248–259. https://doi.org/10.1016/j.foodchem.2019.05.050

Dong, H., & Vasanthan, T. (2020). Amylase resistance of corn, faba bean, and field pea starches as influenced by three different phosphorylation (cross-linking) techniques. *Food Hydrocolloids, 101*, 105506. https://doi.org/10.1016/j.foodhyd.2019.105506

Dou, H., Jung, E. C., & Lee, S. (2015). Factors affecting measurement of channel thickness in asymmetrical flow field-flow fractionation. *Journal of Chromatography A, 1393*, 115–121. https://doi.org/10.1016/j.chroma.2015.03.025

Dou, H., Lee, Y. J., Jung, E. C., Lee, B. C., & Lee, S. (2013). Study on steric transition in asymmetrical flow field-flow fractionation and application to characterization of high-energy material. *Journal of Chromatography A, 1304*, 211–219. https://doi.org/10.1016/j.chroma.2013.06.051

Dou, H., Zhou, B., Jang, H. D., & Lee, S. (2014). Study on antidiabetic activity of wheat and barley starch using asymmetrical flow field-flow fractionation coupled with multiangle light scattering. *Journal of Chromatography A, 1340*, 115–120. https://doi.org/10.1016/j.chroma.2014.03.014

Doyle, L., & Wang, M. (2019). Overview of extracellular vesicles, their origin, composition, purpose, and methods for exosome isolation and analysis. *Cells, 8*(7), Article 727. https://doi.org/10.3390/cells8070727

Englyst, H. N., Kingman, S. M., & Cummings, J. H. (1992). Classification and measurement of nutritionally important starch fractions. *European Journal of Clinical Nutrition, 46*(Suppl. 2), S33–S50. https://doi.org/10.1128/IAI.01649-06

Evans, A. (2016). Resistant starch and health. *Encyclopedia of Food Grains (Second Edition)*, 230–235. https://doi.org/10.1016/B978-0-12-394437-5.00097-8

Faucard, P., Grimaud, F., Lourdin, D., Maigret, J. E., Moulis, C., Remaud-Siméon, M., & Rolland-Sabaté, A. (2018). Macromolecular structure and film properties of enzymatically-engineered high molar mass dextrans. *Carbohydrate Polymers, 181*, 337–344. https://doi.org/10.1016/j.carbpol.2017.10.065

Fraunhofer, M. E., Jakob, F., & Vogel, R. F. (2018). Influence of different sugars and initial pH on β-glucan formation by lactobacillus brevis TMW 1.2112. *Current Microbiology, 75*(7), 794–802. https://doi.org/10.1007/s00284-018-1450-z

French, D. (1984). *Organization of starch granules* (Second Edition, pp. 183–247). Starch: Chemistry and Technology. https://doi.org/10.1016/B978-0-12-746270-7.50013-6.

Fuentes, C., Castañeda, R., Rengel, F., Peñarrieta, J. M., & Nilsson, L. (2019a). Characterization of molecular properties of wheat starch from three different types of breads using asymmetric flow field-flow fractionation (AF4). *Food Chemistry, 298*, Article 125090. https://doi.org/10.1016/j.foodchem.2019.125090

Fuentes, C., Choi, J., Wahlgren, M., & Nilsson, L. (2023). Charge and zeta-potential distribution in starch modified with octenyl succinic anhydride (OSA) determined using electrical asymmetrical flow field-flow fractionation (EAF4). *Colloids and Surfaces A: Physicochemical and Engineering Aspects, 657*, Article 130570. https://doi.org/10.1016/j.colsurfa.2022.130570

Fuentes, C., Choi, J., Zielke, C., Peñarrieta, J. M., Lee, S., & Nilsson, L. (2019). Comparison between conventional and frit-inlet channels in separation of

biopolymers by asymmetric flow field-flow fractionation. *Analyst, 144*(15), 4559–4568. https://doi.org/10.1039/c9an00466a
Fuentes, C., Saari, H., Choi, J., Lee, S., Sjoo, M., Wahlgren, M., & Nilsson, L. (2019b). Characterization of non-solvent precipitated starch using asymmetrical flow field-flow fractionation coupled with multiple detectors. *Carbohydrate Polymers, 206*, 21–28. https://doi.org/10.1016/j.carbpol.2018.10.100
Gallant, D. J., Bouchet, B., Buléon, A., & Pérez, S. (1992). Physical characteristics of starch granules and susceptibility to enzymatic degradation. *European Journal of Clinical Nutrition, 46*(Suppl 2), S3–16.
Giddings, J. C. (1993). Retention (steric) inversion in field-flow fractionation: Practical implications in particle size, density and shape analysis. *Analyst, 118*(12), 1487–1494. https://doi.org/10.1039/an9931801487
Giddings, J. C. (1966). A new separation concept based on a coupling of concentration and flow nonuniformities. *Separation science, 1*(1), 123–125. https://doi.org/10.1080/01496396608049439
Giddings, J. C., Ratanathanawongs, S. K., & Moon, M. H. (1991). Field-flow fractionation: A versatile technology for particle characterization in the size range 10^{-3} to 10^{2} micrometers. *KONA Powder and Particle Journal, 9*, 200–217. https://doi.org/10.14356/kona.1991025
Giddings, J. C., Yang, F. J., & Myers, M. N. (1977). Flow field flow fractionation as a methodology for protein separation and characterization. *Analytical Biochemistry, 81*(2), 395–407. https://doi.org/10.1016/0003-2697(77)90710-2
Gilbert, R. G., Witt, T., & Hasjim, J. (2013). What is being learned about starch properties from multiple-level characterization. *Cereal Chemistry, 90*(4), 312–325. https://doi.org/10.1094/CCHEM-11-12-0141-FI
Gong, B., Cheng, L. L., Gilbert, R. G., & Li, C. (2019). Distribution of short to medium amylose chains are major controllers of in vitro digestion of retrograded rice starch. *Food Hydrocolloids, 96*, 634–643. https://doi.org/10.1016/j.foodhyd.2019.06.003
González-Espinosa, Y., Sabagh, B., Moldenhauer, E., Clarke, P., & Goycoolea, F. M. (2019). Characterisation of chitosan molecular weight distribution by multi-detection asymmetric flow-field flow fractionation (AF4) and SEC. *International Journal of Biological Macromolecules, 136*, 911–919. https://doi.org/10.1016/j.ijbiomac.2019.06.122
Guisbiers, G., Wang, Q., Khachatryan, E., Mimun, L., Mendoza-Cruz, R., Larese-Casanova, P., & Nash, K. (2016). Inhibition of E. coli and S. aureus with selenium nanoparticles synthesized by pulsed laser ablation in deionized water. *International Journal of Nanomedicine, 11*, 3731–3736. https://doi.org/10.2147/ijn.s106289
Guo, P., Li, Y., An, J., Shen, S., & Dou, H. (2019). Study on structure-function of starch by asymmetrical flow field-flow fractionation coupled with multiple detectors: A review. *Carbohydrate Polymers, 226*, Article 115330. https://doi.org/10.1016/j.carbpol.2019.115330
Guo, Y., Zhang, W., Sun, Y., Ye, H., Shen, S., & Dou, H. (2022). Asymmetrical flow field-flow fractionation combined with liquid chromatography enables rapid, quantitative, and structurally informative detection of resistant starch. *Microchemical Journal, 181*, Article 107787. https://doi.org/10.1016/j.microc.2022.107787
Haq, F., Yu, H., Wang, L., Teng, L., Haroon, M., Khan, R. U., & Nazir, A. (2019). Advances in chemical modifications of starches and their applications. *Carbohydrate Research, 476*, 12–35. https://doi.org/10.1016/j.carres.2019.02.007
Hernandez-Hernandez, O., Julio-Gonzalez, L. C., Doyagüez, E. G., & Gutiérrez, T. J. (2023). Potentially health-promoting spaghetti-type pastas based on doubly modified corn starch: starch oxidation via wet chemistry followed by organocatalytic butyrylation using reactive extrusion. *Polymers, 15*(7), 1704. https://doi.org/10.3390/polym15071704
Imberty, A., Chanzy, H., Pérez, S., Buléon, A., & Tran, V. (1987). Three-dimensional structure analysis of the crystalline moiety of A-starch. *Food Hydrocolloids, 1*(5), 455–459. https://doi.org/10.1016/S0268-005X(87)80040-1
Joensson, J. A., & Carlshaf, A. (1989). Flow field flow fractionation in hollow cylindrical fibers. *Analytical Chemistry, 61*(1), 11–18. https://doi.org/10.1021/ac00176a004
Kammer, F., Legros, S., Hofmann, T., Larsen, E. H., & Loeschner, K. (2011). Separation and characterization of nanoparticles in complex food and environmental samples by field-flow fractionation. *TRAC Trends in Analytical Chemistry, 30*(3), 425–436. https://doi.org/10.1016/j.trac.2010.11.012
Kang, D., & Moon, M. H. (2004). Miniaturization of frit inlet asymmetrical flow field-flow fractionation. *Analytical Chemistry, 76*(13), 3851–3855. https://doi.org/10.1021/ac0496704
Kim, Y. B., Yang, J. S., & Moon, M. H. (2018). Investigation of steric transition with field programming in frit inlet asymmetrical flow field-flow fractionation. *Journal of Chromatography A, 1576*, 131–136. https://doi.org/10.1016/j.chroma.2018.09.036
Lee, S., Kim, S. T., Pant, B. R., Kwen, H. D., Song, H. H., Lee, S. K., & Nehete, S. V. (2010). Carboxymethylation of corn starch and characterization using asymmetrical flow field-flow fractionation coupled with multiangle light scattering. *Journal of Chromatography A, 1217*(27), 4623–4628. https://doi.org/10.1016/j.chroma.2010.04.082
Leeman, M., Islam, M. T., & Haseltine, W. G. (2007). Asymmetrical flow field-flow fractionation coupled with multi-angle light scattering and refractive index detections for characterization of ultra-high molar mass poly(acrylamide) flocculants. *Journal of Chromatography A, 1172*(2), 194–203. https://doi.org/10.1016/j.chroma.2007.10.006
Li, C., Li, H., & Gilbert, R. G. (2019). Characterizing starch molecular structure of rice. *Rice Grain Quality, 1892*, 169–185. https://doi.org/10.1007/978-1-4939-8914-0_10
Liang, T., Xie, X., Wu, L., Li, L., Yang, L., Jiang, T., & Wu, Q. (2023). Metabolism of resistant starch RS3 administered in combination with Lactiplantibacillus plantarum strain 84–3 by human gut microbiota in simulated fermentation experiments in vitro and in a rat model. *Food Chemistry, 411*, Article 135412. https://doi.org/10.1016/j.foodchem.2023.135412
Litzen, A. (1993). Separation speed, retention, and dispersion in asymmetrical flow field-flow fractionation as functions of channel dimensions and flow rates. *Analytical Chemistry, 65*(4), 461–470. https://doi.org/10.1021/ac00052a025
Litzen, A., & Wahlund, K. G. (1991). Zone broadening and dilution in rectangular and trapezoidal asymmetrical flow field-flow fractionation channels. *Analytical Chemistry, 63*(10), 1001–1007. https://doi.org/10.1021/ac00010a013
Lopez-Silva, M., Bello-Perez, L. A., Castillo-Rodriguez, V. M., Agama-Acevedo, E., & Alvarez-Ramirez, J. (2020). In vitro digestibility characteristics of octenyl succinic acid (OSA) modified starch with different amylose content. *Food Chemistry, 304*, Article 125434. https://doi.org/10.1016/j.foodchem.2019.125434
Lu, K., Zhu, J., Bao, X., Liu, H., Yu, L., & Chen, L. (2020). Effect of starch microstructure on microwave-assisted esterification. *International Journal of Biological Macromolecules, 164*, 2550–2557. https://doi.org/10.1016/j.ijbiomac.2020.08.099
Ma, P. L., Buschmann, M. D., & Winnik, F. M. (2010). One-step analysis of DNA/chitosan complexes by field-flow fractionation reveals particle size and free chitosan content. *Biomacromolecules, 11*(3), 549–554. https://doi.org/10.1021/bm901345q
Ma, Z., Yin, X., Hu, X., Li, X., Liu, L., & Boye, J. I. (2018). Structural characterization of resistant starch isolated from Laird lentils (Lens culinaris) seeds subjected to different processing treatments. *Food Chemistry, 263*, 163–170. https://doi.org/10.1016/j.foodchem.2018.04.122
Magnusson, E., & Nilsson, L. (2011). Interactions between hydrophobically modified starch and egg yolk proteins in solution and emulsions. *Food Hydrocolloids, 25*(4), 764-772. https://doi.org /10.1016/j.foodhyd.2010.09.006.
Mélin, C., Perraud, A., Akil, H., Jauberteau, M. O., Cardot, P., Mathonnet, M., & Battu, S. (2012). Cancer stem cell ssorting from colorectal cancer cell lines by sedimentation field flow fractionation. *Analytical Chemistry, 84*(3), 1549–1556. https://doi.org/10.1021/ac202797z
Moon, M. H., & Giddings, J. C. (1992). Extension of sedimentation/steric field-flow fractionation into the submicrometer range: Size analysis of 0.2-15-μm metal particles. *Analytical Chemistry, 64*(23), 3029–3037. https://doi.org/10.1021/ac00047a027
Mudalige, T. K., Qu, H., Sánchez-Pomales, G., Sisco, P. N., & Linder, S. W. (2015). Simple functionalization strategies for enhancing nanoparticle separation and recovery with asymmetric flow field flow fractionation. *Analytical Chemistry, 87*(3), 1764–1772. https://doi.org/10.1021/ac503683n
Myers, M. N., & Giddings, J. C. (1982). Properties of the transition from normal to steric field-flow fractionation. *Analytical Chemistry, 54*(13), 2284–2289. https://doi.org/10.1021/ac00250a032
Nilsson, L. (2013). Separation and characterization of food macromolecules using field-flow;fractionation: A review. *Food Hydrocolloids, 30*(1), 1–11. https://doi.org/10.1016/j.foodhyd.2012.04.007
Panyoo, A. E., & Emmambux, M. N. (2017). Amylose-lipid complex production and potential health benefits: A mini-review. *Starch - Stärke, 69*(7–8), Article 1600203. https://doi.org/10.1002/star.201600203
Perez-Rea, D., Zielke, C., & Nilsson, L. (2017). Co-elution effects can influence molar mass determination of large macromolecules with asymmetric flow field-flow fractionation coupled to multiangle light scattering. *Journal of Chromatography A, 1506*, 138–141. https://doi.org/10.1016/j.chroma.2017.05.029
Podzimek, S. (2012). Asymmetric flow field flow fractionation. *Encyclopedia of Analytical Chemistry, 1–19*. https://doi.org/10.1002/9780470027318.a9289
Ratanathanawongs Williams, S. K., & Lee, D. (2006). Field-flow fractionation of proteins, polysaccharides, synthetic polymers, and supramolecular assemblies. *Journal of Separation Science, 29*(12), 1720–1732. https://doi.org/10.1002/jssc.200600151
Reschiglian, P., Melucci, D., Zattoni, A., Malló, L., Hansen, M., Kummerow, A., & Miller, M. (2000). Working without accumulation membrane in flow field-flow fractionation. *Analytical Chemistry, 72*(24), 5945–5954. https://doi.org/10.1021/ac000608q
Rolland-Sabaté, A., Guilois, S., Jaillais, B., & Colonna, P. (2011). Molecular size and mass distributions of native starches using complementary separation methods: Asymmetrical flow field flow fractionation (A4F) and hydrodynamic and size exclusion chromatography (HDC-SEC). *Analytical and Bioanalytical Chemistry, 399*(4), 1493–1505. https://doi.org/10.1007/s00216-010-4208-4
Schimpf, M. E., Caldwell, K., & Giddings, J. C. (2000). *Field flow fractionation handbook*. New York: Wiley-Interscience.
Schimpf, M. E., Myers, M. N., & Giddings, J. C. (1987). Measurement of polydispersity of ultra-narrow polymer fractions by thermal field-flow fractionation. *Journal of Applied Polymer Science, 33*(1), 117–135. https://doi.org/10.1002/app.1987.070330111
Song, T., Zhang, W., Chen, X., Zhang, A., Guo, S., Shen, S., & Dou, H. (2021). Insights into the correlations between the size of starch at nano- to microscale and its functional properties based on asymmetrical flow field-flow fractionation. *International Journal of Biological Macromolecules, 193*, 500–509. https://doi.org/10.1016/j.ijbiomac.2021.10.090
Tekin, T., & Dincer, E. (2023). Effect of resistant starch types as a prebiotic. *Applied Microbiology and Biotechnology, 107*(2–3), 491–515. https://doi.org/10.1007/s00253-022-12325-y
Tester, R. F., Karkalas, J., & Qi, X. (2004). Starch—composition, fine structure and architecture. *Journal of Cereal Science, 39*(2), 151–165. https://doi.org/10.1016/j.jcs.2003.12.001
Thongsomboon, W., Srihanam, P., & Baimark, Y. (2023). Preparation of flexible poly(l-lactide)-b-poly(ethylene glycol)-b-poly(l-lactide)/talcum/thermoplastic starch ternary composites for use as heat-resistant and single-use bioplastics. *International Journal of Biological Macromolecules, 230*, Article 123172. https://doi.org/10.1016/j.ijbiomac.2023.123172
Wahlund, K. G. (2013). Flow field-flow fractionation: Critical overview. *Journal of Chromatography A, 1287*, 97–112. https://doi.org/10.1016/j.chroma.2013.02.028

Wahlund, K. G., & Giddings, J. C. (1987). Properties of an asymmetrical flow field-flow fractionation channel having one permeable wall. *Analytical Chemistry, 59*(9), 1332–1339. https://doi.org/10.1021/ac00136a016

Wahlund, K. G., Leeman, M., & Santacruz, S. (2011). Size separations of starch of different botanical origin studied by asymmetrical-flow field-flow fractionation and multiangle light scattering. *Analytical and Bioanalytical Chemistry, 399*(4), 1455–1465. https://doi.org/10.1007/s00216-010-4438-5

Wahlund, K. G., Winegarner, H. S., Caldwell, K. D., & Giddings, J. C. (1986). Improved flow field-flow fractionation system applied to water-soluble polymers: Programming, outlet stream splitting, and flow optimization. *Analytical Chemistry, 58*(3), 573–578. https://doi.org/10.1021/ac00294a018

Wang, S., Zuo, Z., Wang, Q., Zhou, A., Wang, G., Xu, G., & Zou, J. (2023). Replacing starch with resistant starch (Laminaria japonica) improves water quality, nitrogen and phosphorus budget and microbial community in hybrid snakehead (Channa maculata ♀ × Channa argus ♂). *Water Environment Research, 95*(2), Article e10836. https://doi.org/10.1002/wer.10836

Wen, J. J., Li, M. Z., & Nie, S. P. (2023). Dietary supplementation with resistant starch contributes to intestinal health. *Current Opinion in Clinical Nutrition and Metabolic Care, 26*(4), 334–340. https://doi.org/10.1097/mco.0000000000000939

Wittgren, B., Wahlund, K. G., Andersson, M., & Arfvidsson, C. (2002). Polysaccharide characterization by flow field-flow fractionation-multiangle light scattering: Initial studies of modified starches. *International Journal of Polymer Analysis and Characterization, 7*(1–2), 19–40. https://doi.org/10.1080/10236660214599

Wu, Z., Zhao, W., Yin, Y., Wei, Y., Liu, Y., Zhu, N., & Liu, J. (2023). Separation and characterization of biomacromolecules, bionanoparticles, and biomicroparticles using flow field-flow fractionation: Current applications and prospects. *TrAC Trends in Analytical Chemistry, 164*, Article 117114. https://doi.org/10.1016/j.trac.2023.117114

Yee, J., Roman, L., Pico, J., Aguirre-Cruz, A., Bello-Perez, L. A., Bertoft, E., & Martinez, M. M. (2021). The molecular structure of starch from different Musa genotypes: Higher branching density of amylose chains seems to promote enzyme-resistant structures. *Food Hydrocolloids, 112*, Article 106351. https://doi.org/10.1016/j.foodhyd.2020.106351

Yoo, Y., Choi, J., Zielke, C., Nilsson, L., & Lee, S. (2017). Fluorescence-labelling for analysis of protein in starch using asymmetrical flow field-flow fractionation (AF4). *Analytical Science and Technology, 30*(1), 1–9. https://doi.org/10.5806/ast.2017.30.1.1

Zattoni, A., Rambaldi, D. C., Casolari, S., Roda, B., & Reschiglian, P. (2011). Tandem hollow-fiber flow field-flow fractionation. *Journal of Chromatography A, 1218*(27), 4132–4137. https://doi.org/10.1016/j.chroma.2011.02.051

Zhang, W., Shen, S., Song, T., Chen, X., Zhang, A., & Dou, H. (2021). Insights into the structure and conformation of potato resistant starch (type 2) using asymmetrical flow field-flow fractionation coupled with multiple detectors. *Food Chemistry, 349*, Article 129168. https://doi.org/10.1016/j.foodchem.2021.129168

Zhang, W., Wang, J., Guo, P., Dai, S., Zhang, X., Meng, M., & Dou, H. (2019). Study on the retrogradation behavior of starch by asymmetrical flow field-flow fractionation coupled with multiple detectors. *Food Chemistry, 277*, 674–681. https://doi.org/10.1016/j.foodchem.2018.11.033

Zhu, F., & Liu, P. (2020). Starch gelatinization, retrogradation, and enzyme susceptibility of retrograded starch: Effect of amylopectin internal molecular structure. *Food Chemistry, 316*, Article 126036. https://doi.org/10.1016/j.foodchem.2019.126036

Zielke, C., Fuentes, C., Piculell, L., & Nilsson, L. (2018). Co-elution phenomena in polymer mixtures studied by asymmetric flow field-flow fractionation. *Journal of Chromatography A, 1532*, 251–256. https://doi.org/10.1016/j.chroma.2017.12.028